

## Mechanical Strength Analysis of Fiber-Reinforced Geopolymer Nanocomposite

Shahir Ahmad Safi<sup>\*1</sup>, Ali Raza<sup>1</sup>, Mujib Ul Rahman Rahmani<sup>1</sup>, Zekrullah Jamali<sup>1</sup> and Abdellatif Selmi<sup>2</sup>

<sup>1</sup>Department of Civil Engineering, University of Engineering and Technology Taxila, 47050, Pakistan

<sup>2</sup>Department of Civil Engineering, Prince Sattam Bin Abdulaziz University, Alkharj, 11942, Saudi Arabia

\*([shahirahmad229@gmail.com](mailto:shahirahmad229@gmail.com))

(Received: 18 November 2024, Accepted: 26 November 2024)

(2nd International Conference on Trends in Advanced Research ICTAR 2024, November 22-23, 2024)

**ATIF/REFERENCE:** Safi, S. A., Raza, A., Rahmani, M. U. R., Jamali, Z. & Selmi, A. (2024). Mechanical Strength Analysis of Fiber-Reinforced Geopolymer Nanocomposite. *International Journal of Advanced Natural Sciences and Engineering Researches*, 8(10), 238-242.

**Abstract** – Engineered geopolymer composites (EGC) are emerging as a sustainable alternative to traditional cement-based materials, like engineered cementitious composites (ECC). Unlike Portland cement, which has a significant environmental impact, EGC reduces energy use, carbon emissions, and environmental damage. Recent developments have produced stronger, more flexible, and eco-friendly EGC. While EGC with GGBS (Ground Granulated Blast Furnace Slag) exhibits similar mechanical properties to Portland cement, it tends to crack under stress. This study improves the ductility of GGBS-EGC by incorporating polyethylene (PE) fibers and functionalized multi-walled carbon nanotubes (f-MWCNTs). Mechanical testing of compositions with 0.10% f-MWCNTs and 0.15% PE fibers showed a strength of 3.71 MPa under tension, elongation of 5.48%, initial tensile fracture strength of 2.46 MPa, and compressive strength of 38.03 MPa after 28 days. The PSH index for GGBS-EGC2 was 32.67, demonstrating excellent ductility and multiple cracking.

**Keywords** – Geopolymer, Multi-Walled Carbon Nanotubes, Compressive Strength, Tensile Strength.

### I. INTRODUCTION

Ordinary Portland cement, a highly effective hydraulic binder, is extensively used but its production process releases nitrogen oxides, sulfides, and carbides, significantly contributing to carbon pollution. Geopolymer, introduced by Davidovits in 1978 [1], is a cementitious material that does not depend on Portland cement. As an eco-friendly alternative, geopolymer has recently become a subject of debate [2-7]. Compared to Portland cement, geopolymer can reduce CO<sub>2</sub> emissions by 80% and energy consumption by 60% [8].

The mechanical properties of geopolymers, such as tensile and compressive strength, elongation, ductility, and durability, can be enhanced by incorporating various fibers [9-12]. However, long fibers can complicate the mixing process as they may not fully integrate into the aluminosilicate materials. Research by Lin et al. suggests that short fibers can improve the ductility of geopolymers [13]. Mechanical testing has identified optimal fiber blend ratios. Adding fibers with low elastic moduli to engineered geopolymer composites (EGCs) can reduce tensile strength but improve ductility. These fibers can include polypropylene (PP), steel, polyethylene (PE), among others [14, 15]. While fiber addition can enhance the

ductility of GGBS-EGC, further research is required to determine the optimal fiber types and quantities. This study focuses on using PE fibers and functionalized multi-walled carbon nanotubes (f-MWCNTs) to improve the ductility of GGBS-EGC. Samples were prepared and cured, materials were sourced, and an orthogonal experiment was conducted to adjust PE fiber and f-MWCNT doses. Compressive strength was measured through uniaxial compression testing. The impact of Ca<sup>2+</sup> and f-MWCNTs on compressive strength trends was analyzed, and tensile properties such as elongation at break, initial cracking stress, and ultimate tensile strength were assessed.

## II. MATERIALS AND METHOD

### i. Materials

Fly ash (FA), rich in silicon and aluminum, was utilized in this study, with some of it substituted by GGBS. Figure 1 displays images of the raw materials (SF, GGBS, MK, and PE fiber). GGBS is yellow-brown and contains sand-like particles. To enhance the compatibility and dispersion of the selected f-MWCNTs in solvents. The f-MWCNTs appear as black powder and are characterized by a fibrous, elongated structure with some curvature, as observed through SEM with EFSM. The ends of f-MWCNTs are often flat rather than conical. They have a strength ranging from 64 to 92 GPa under tension and a Young's modulus of 120 GPa, as detailed in Table 1. The NaOH used is a white, spherical solid with 8.75% Na<sub>2</sub>O, 27.7% SiO<sub>2</sub>, and 63.55% water content. It is a Na<sub>2</sub>SiO<sub>3</sub> solution with a modulus ratio of 3.24 and a water-to-solid ratio of 1:5.

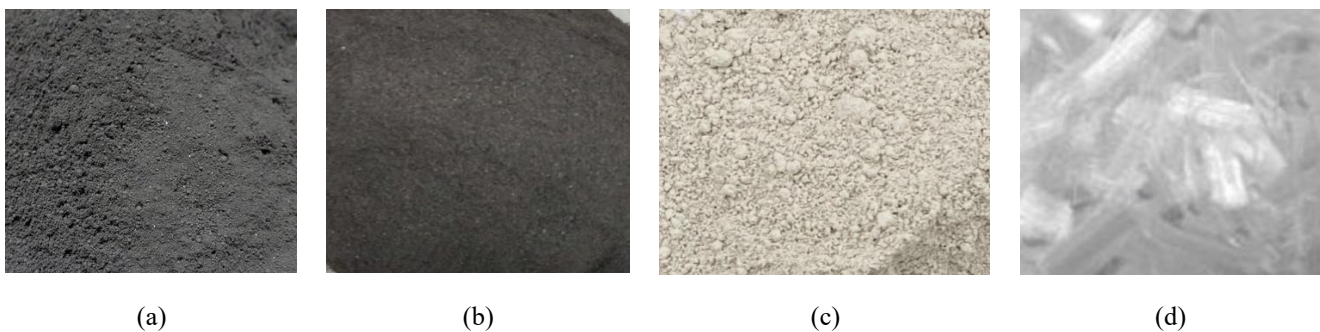


Figure 1. Raw materials (a) SF (b) GGBS (c) MK (d) PE fiber

Table 1. Features of f-MWCNTs

Property	Value
Length	5-20μm
Young's modulus	120 GPa
Surface area	160-210 m <sup>2</sup> /g
Purity	Greater than 95
Outside diameter	10-30 nm
Density	0.06-0.10 g/cm <sup>3</sup>
Resistivity	< 2100 μΩ.m
Carboxyl content	>0.5 mmol/g

### ii. Preparation and Testing of Specimens

To prepare the alkaline activator, mix solid, spherical sodium hydroxide (99% purity) with sodium silicate solution (modulus 3.24) using a glass rod. Stir for eight minutes till NaOH is fully dissolved. Let the mixture cool to room temperature and become clear. This alkaline activator enhances the geopolymer's resistance to cracking. Next, combine f-MWCNTs and SDS dispersant in water and mix for five to six minutes. Ultrasonicate the mixture for 25 minutes at 62°C to ensure proper mixing of f-MWCNTs. Then, blend SF, FA, quartz sand, GGBS, and metakaolin (MK) in a mixer at low speed for three to five minutes. Add the alkaline activator and mix for an additional three minutes. Incorporate the sonicated f-MWCNT solution

and stir vigorously for five minutes. Finally, add PE fibers. Once the geopolymer and PE fibers are well-mixed, pour the material into molds coated with a release agent. Allow the specimens to set for 24 hours at room temperature before curing in a chamber at 25°C and over 90% relative humidity for 28 days.

Orthogonal experiments will use the three dependent variables listed in Table 2 to determine the optimal FA replacement ratio with GGBS and the best f-MWCNTs and PE fiber proportions for the final geopolymer. Three experimental groups will be tested in parallel for compressive strength, with six groups for axial tensile stress and single-edge notched stress tests, and four groups for three-point bending tests.

Table 2. Dependent parameters in tests.

Sample ID	PE fiber (vol %)	f-MWCNTs (mass %)	GGBS substitution (mass %)
GGBS-SGC1	0.15	0.05	10
GGBS-SGC2	0.15	0.10	20
GGBS-SGC3	0.15	0.15	30
GGBS-SGC4	0.2	0.05	20
GGBS-SGC5	0.2	0.10	30
GGBS-SGC6	0.2	0.15	10
GGBS-SGC7	0.25	0.05	30
GGBS-SGC8	0.25	0.10	10
GGBS-SGC9	0.25	0.15	20

### III. RESULTS AND DISCUSSION

#### i. Compressive Strength

The optimal mix—0.15% PE fiber, 0.10% f-MWCNTs, and 20% GGBS substitution—yields a compressive strength 1.16 times that of standard Portland cement, reaching up to 38.03 MPa. This demonstrates that replacing FA with GGBS significantly enhances compressive strength. A 20% GGBS replacement improves the internal structure of GGBS-EGC by reducing porosity due to the calcium oxide, silicon dioxide, and aluminum oxide in GGBS. This structural enhancement leads to increased material density and strength. The improved compressive strength is partially due to the reaction of  $\text{Ca}^{2+}$  in GGBS with aluminosilicates, forming stable compounds like calcium aluminosilicate and calcium silicate. Additionally, the alkaline environment facilitates the formation of cementitious materials containing calcium and accelerates the nucleation and setting processes. The transformation of N-A-S-H gel into stronger C-A-S-H and C-S-H gels in GGBS-EGC is also promoted by the presence of  $\text{Ca}^{2+}$  [16]. Figure 2 illustrates the compressive strengths of various mixes. The impact of GGBS replacement on compressive performance surpasses that of PE fibers and f-MWCNTs. Beyond a 20% GGBS replacement, compressive strength declines due to excessive  $\text{Ca}^{2+}$  causing gaps between silicon dioxide and aluminum oxide, which weakens the internal structure and reduces chemical stability. Ideal f-MWCNTs concentrations enhance compressive strength by dispersing uniformly in the GGBS-EGC matrix, filling pores, and reinforcing the structure. Conversely, excessive f-MWCNTs tend to clump, increasing the internal matrix surface area and decreasing strength. Increasing PE fiber content boosts adhesion and shear flow resistance but can lead to clumping if excessive, potentially causing structural failure and reduced surface area. Therefore, the highest compressive strength of GGBS-EGC is achieved with 0.15% PE fiber, 0.10% f-MWCNTs, and 20% GGBS substitution.

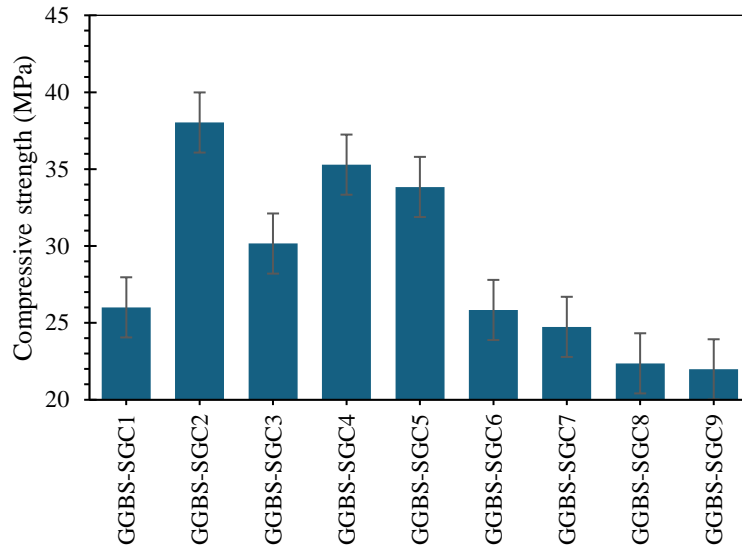


Figure 2. Compressive strength of different mixes

ii. Tensile Strength

The stress-strain curves were obtained through uniaxial tensile tests of GGBS-based composite having f-MWCNTs and PE fibers over a 28-day curing period. These curves, illustrated in Figure 3, exhibit typical variations resulting from stress fluctuations due to crack formation. Measurements were recorded at the initial crack formation and at the ultimate failure points. GGBS-EGC2 and GGBS-EGC3 showed 49 and 57 cracks, correspondingly, with crack size of 83.76  $\mu\text{m}$  and 76.91  $\mu\text{m}$ , elongations of 5.13% and 5.48%, and crack sizes of 1.45 mm and 1.63 mm. Each sample had an average crack width of less than 110  $\mu\text{m}$ . Smaller cracks in GGBS-EGC indicate better durability. Aluminum silicate, a key component in GGBS-EGC, plays a critical role in crack prevention and stress support [17]. GGBS-EGC2 displays higher elongation, initial cracking stress, and ultimate cracking stress compared to PE-EGC, demonstrating that f-MWCNTs enhance the tensile strength of GGBS-EGC. However, GGBS-EGC2 generally exhibits lower compressive and tensile strengths compared to UHEGC, attributed to GGBS's lower reactivity [18].

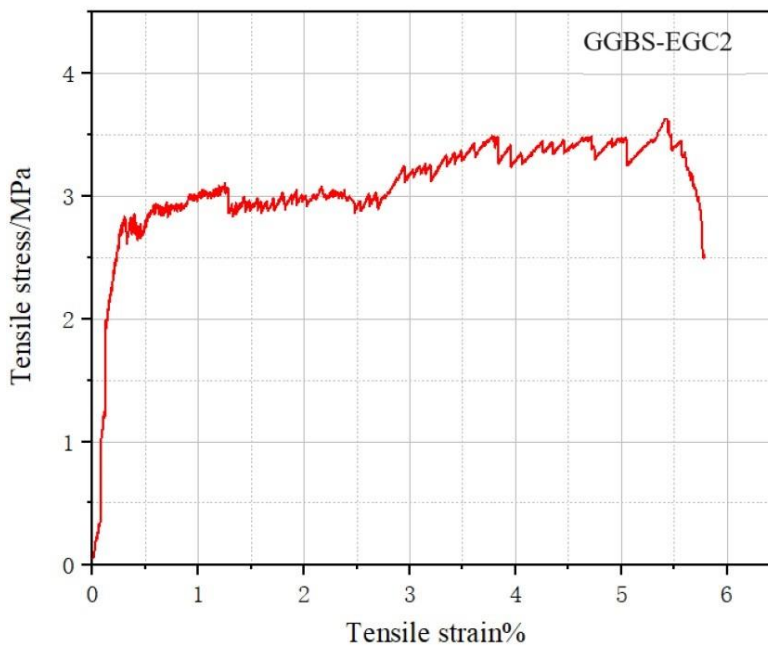


Figure 3. Stress-Strain Curve of Uniaxial Tensile Test.

#### IV. CONCLUSIONS

Key findings include:

1. After 28 days of curing, the GGBS-based engineering geopolymer achieved a compressive strength of 38.03 MPa. It exhibited an initial tensile fracture strength of 2.46 MPa, a peak tensile strength of 3.71 MPa, and 5.48% elongation. Uniaxial tensile testing highlighted the geopolymer's plastic properties, with crack spacings up to 1.45 mm and crack size of 76.91  $\mu\text{m}$ , all samples showing crack widths under 110  $\mu\text{m}$ .

2. The classical PSH (Plasticity and Stability of Hardening) index, evaluated through SENT and three-point bending tests, explained the high ductility of GGBS-EGC. The GGBS-EGC2 sample met energy and strength requirements for strain hardening, with a SHP index of 32.67, surpassing 3, indicating effective multiple cracking. The presence of f-MWCNTs and PE fibers improved tensile behavior by bridging cracks at the fracture surface.

#### REFERENCES

- [1] Davidovits, J., Geopolymers and geopolymeric materials. *Journal of thermal analysis*, 1989. 35: p. 429-441.
- [2] Raza, A., et al., A Comprehensive Review on Material Characterization and Thermal Properties of Geopolymers: Potential of Various Fibers. *Case Studies in Construction Materials*, 2024: p. e03519.
- [3] El Ouni, M.H., et al., Behavior of alkali-activated coal ash basalt fiber-reinforced geopolymer nanocomposite incorporated with nano sodium oxide. *Materials Letters*, 2023. 335: p. 133850.
- [4] Raza, A., et al., Mechanical Performance of Geopolymer Composites Containing Nano-Silica and Micro-Carbon Fibers. *Arabian Journal for Science and Engineering*, 2022: p. 1-12.
- [5] Raza, A., et al., Experimental study on mechanical, toughness and microstructural characteristics of micro-carbon fibre-reinforced geopolymer having nano TiO<sub>2</sub>. *Alexandria Engineering Journal*, 2022.
- [6] Alvee, A.R., et al., Experimental study of the mechanical properties and microstructure of geopolymer paste containing nano-silica from agricultural waste and crystalline admixtures. *Case Studies in Construction Materials*, 2022. 16: p. e00792
- [7] El Ouni, M.H., et al., Enhancement of mechanical and toughness properties of carbon fiber-reinforced geopolymer pastes comprising nano calcium oxide. *Journal of the Australian Ceramic Society*, 2022: p. 1-13.
- [8] Oderji, S.Y., et al., Fresh and hardened properties of one-part fly ash-based geopolymer binders cured at room temperature: Effect of slag and alkali activators. *Journal of Cleaner Production*, 2019. 225: p. 1-10.
- [9] Zhang, P., et al., Effect of PVA fiber on properties of geopolymer composites: A comprehensive review. *Journal of Materials Research and Technology*, 2024.
- [10] Chen, K.-y., et al., Performance characteristics of micro fiber-reinforced ambient cured one-part geopolymer mortar for repairing. *Construction and Building Materials*, 2024. 415: p. 135086.
- [11] Zhang, D., et al., Engineering and microstructural properties of carbon-fiber-reinforced fly-ash-based geopolymer composites. *Journal of Building Engineering*, 2023. 79: p. 107883.
- [12] Jegan, M., R. Annadurai, and P.K. Rajkumar, A state of the art on effect of alkali activator, precursor, and fibers on properties of geopolymer composites. *Case Studies in Construction Materials*, 2023. 18: p. e01891.
- [13] Lin, T., et al., Effects of fiber length on mechanical properties and fracture behavior of short carbon fiber reinforced geopolymer matrix composites. *Materials Science and Engineering: A*, 2008. 497(1-2): p. 181-185.
- [14] Raza, A., et al., Microstructural and Thermal Characterization of Polyethylene Fiber-Reinforced Geopolymer Composites. *Journal of Building Engineering*, 2024: p. 109904.
- [15] Raza, A., et al., Mechanical, durability and microstructural characterization of cost-effective polyethylene fiber-reinforced geopolymer concrete. *Construction and Building Materials*, 2024. 432: p. 136661.
- [16] García-Lodeiro, I., et al., Compatibility studies between NASH and CASH gels. Study in the ternary diagram Na<sub>2</sub>O–CaO–Al<sub>2</sub>O<sub>3</sub>–SiO<sub>2</sub>–H<sub>2</sub>O. *Cement and Concrete Research*, 2011. 41(9): p. 923-931.
- [17] Lepech, M.D. and V.C. Li, Application of ECC for bridge deck link slabs. *Materials and Structures*, 2009. 42: p. 1185-1195.
- [18] Li, M., et al., The effects of lithium slag on microstructure and mechanical performance of metakaolin-based geopolymers designed by response surface method (RSM). *Construction and Building Materials*, 2021. 299: p. 123950.